Determination of the Biological Variability of Porcine Explant Tissue in Retinal Damage Ex-vivo Experiments with Optical Laser Radiation

Marc Herbst[a,b], Annette Frederiksen[a], and Wilhelm Stork[b]

[a]Cross-Domain Computing Solutions, Robert Bosch GmbH, Herrenwiesenweg 24, Schwieberdingen, 71701, Germany
[b]Karlsruher Institute of Technology, Institute for Information Processing Technologies, Engesserstraße 5, Karlsruhe, 76131, Germany

ABSTRACT

Laser systems are classified with respect to laser safety. Defined emission limits can be used for this purpose. These emission limits and the rulesets in the international laser safety standard IEC 60825-1:2014 are based on scientific evidence from damage threshold experiments and simulations. However, available data sets of laser-induced damage experiments for specific parameter spaces are limited. Therefore, further determination of damage thresholds for optical laser systems, operating in these parameter spaces, is crucial.

Retinal damage thresholds can be determined with ex-vivo explant experiments, in which animal tissue is irradiated with optical setups. In this context, pulsed laser radiation is used in the optical damage measurement setup and beam profiles of constant irradiance are shaped in this work.

Major factors, influencing the damage thresholds, such as the focusing, the evaluation methods, damage criteria and the biological variability, are identified. The (biological) variability in between the porcine tissue samples is investigated by listing, minimizing and estimating the impact of the influencing factors of ex-vivo experiments. Therefore, single, nano second pulsed experiments at a wavelength of 532 nm are performed. The influence of the biological variability together with the focusing is determined by using two statistical methods, one evaluating all data in a single dose-response curve and the other evaluating all samples individually. The ED_{50} values of the individual sample evaluation spread between 6.51 and 12.42 µJ, resulting in an estimated total variability of ±26.58 % and ±26.32 % for the biological variability together with the focusing in respect to the mean value.

Keywords: Laser tissue interaction, laser safety, eye safety, retinal damage thresholds, ex-vivo explant experiments, ED_{50}, dose-response data, variability, uncertainty, beam shaping, focusing, porcine

1. INTRODUCTION

Optical scanning technologies and laser products, such as Lidar sensors, are reviewed and tested with regard to laser safety for safe use. Products emitting optical radiation in the wavelength range of 400 nm up to 1400 nm pose a potential risk for retinal damage, since the radiation is focused on the retina (Fig. 1). Therefore, to ensure laser safety of laser products, manufacturers use the laser safety standard IEC 60825-1:2014.[1] This laser safety standard specifies maximum accessible emission limits permitted within a particular laser class and provides evaluations methods. The limits provided in the laser safety standard are based on damage thresholds empirically determined in experiments[2,3] and simulations. Therefore, researchers perform and have performed in-vivo experiments mostly on non-human primates (NHP)[4–9] or rabbits[10–12] and ex-vivo experiments with animal tissue such as porcine[13–15] or bovine[16,17] tissue in the past.[2,3,18–21]

However, novel optical scanning technologies, such as Lidar sensors or laser projection systems, feature complex architectures with e.g. beam deflection by several optical elements.[22–25] Due to these complex or scanning

Further author information: (Send correspondence to Marc Herbst)
Marc Herbst: E-mail: marc.herbst@de.bosch.com, marc.herbst@partner.kit.edu, Telephone: +49 711 811 48962

Laser Beam Shaping XXIII, edited by Angela Dudley, Alexander V. Laskin, Proc. of SPIE Vol. 12667, 126670E · © The Authors. Published under a Creative Commons Attribution CC-BY 3.0 License · doi: 10.1117/12.2676827

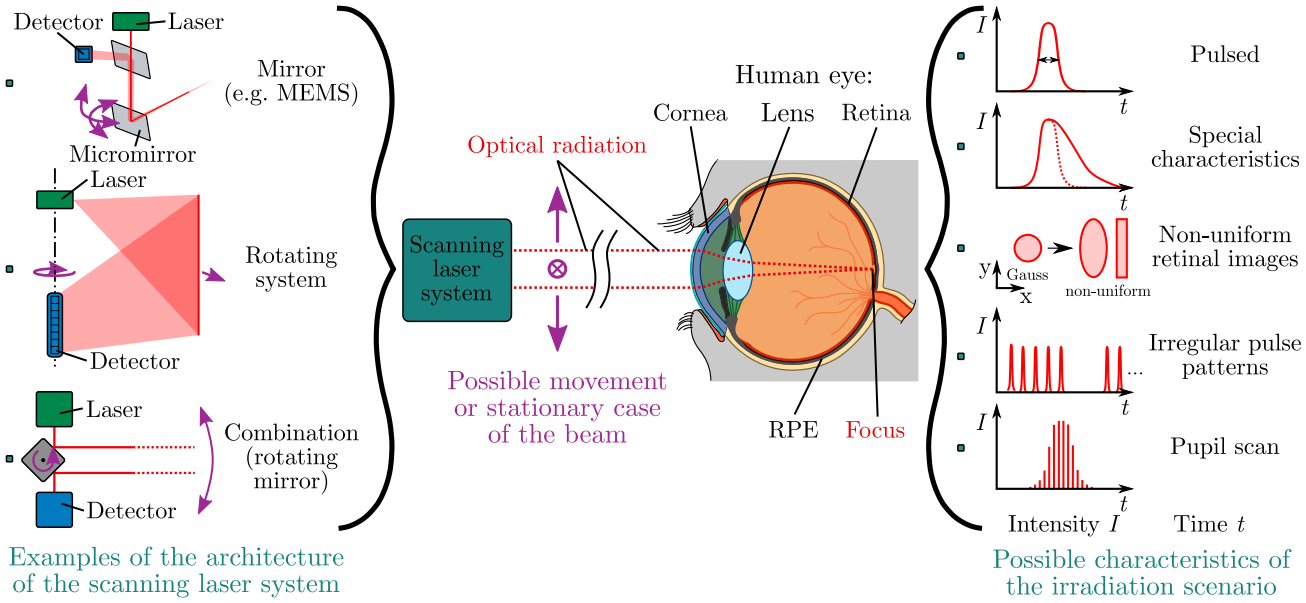

Figure 1. The radiation of optical scanning laser systems focuses on the retina due to the anatomical structures of the human eye. Thereby, a potential risk for retinal damage results. There are different possible characteristics of the irradiation scenario resulting, because of the architecture of the scanning laser system and special cases, if the laser beam of the scanning system is moved.

architectures of laser products, complex irradiation scenarios result, which may be irregularly pulsed, have non-uniform geometries of retinal images[26,27] or 'time varying retinal images'[28] due to the scanning principle (Fig. 1). The laser safety standard covers complex irradiation scenarios for example by reducing complex cases to standard cases, e.g. for elongated geometry of the retinal image. Parts of these complex irradiation scenarios can be modeled by simulations, e.g. thermal damage of non-uniform retinal images.[26] But little to no measurement results exist for many special parameter cases, such as complex irradiation scenarios mentioned above. From previous experiments, there are retinal damage thresholds for pulsed scenarios[4–6,8,15,29] of different wavelengths and interpolations in the gaps between them, such as an 'action spectrum for retinal thermal injury'.[30] Due to the emergence of new laser technologies, such as laser sources with a wavelength of about 905 nm used for Lidar applications, the data base of retinal damage thresholds for such parameter sets is initially small. Moreover, only the thermal retinal damage mechanism can be modeled in simulations so far[31–33] and the biological effects of laser irradiation to the eye are not fully explored yet. No validated simulation method of the thermodynamic damage mechanism is known, which is assumed to dominate for Lidar applications at high energies in the nano second pulse regime. Until the damage mechanisms are sufficiently understood and can be modeled, it is important to cover these irradiation scenarios of emerging technologies metrologically and to expand the data base for the laser safety standard continuously.

A particularly interesting and ethically attractive method to determine retinal damage thresholds, that does not require experiments with living animals, are ex-vivo experiments with explant tissue. Therefore, in a previous publication by Herbst et al. ,[27] an optical setup for performing ex-vivo explant experiments has been presented. In this publication, elongated retinal spot geometries were addressed, which is an example of complex irradiation scenarios mentioned above. In the course of the experiments, major influencing factors for the ED_{50} values, which were determined in these experiments and represent a 50% probability of damage, have been identified.

In this publication the influencing factors on ex-vivo experiments with optical setups are identified and categorized upon their impact. Therefore, additional measurements with the goal to improve ex-vivo explant experiments are presented in this work, where the influencing factors of the measurement procedure have been minimized. The biological variability of the tissue samples is considered having a major impact on the retinal damage threshold.[3,34] Therefore, to determine the impact of the biological variability of porcine tissue samples,

ex-vivo experiments are performed using the same setup as in the previous study.[27]

2. EX-VIVO EXPERIMENTS TO DETERMINE RETINAL DAMAGE THRESHOLDS

2.1 History and state of the art

Ex-vivo experiments are and have been used in the past in various fields, such as the determination of retinal damage thresholds, research to the retinal damage mechanisms (microcavitation or microbubble formation) and testing of medical applications such as selective retinal therapy (SRT). Table 5 (see appendix) lists all the literature that includes ex-vivo experiments of retinal damage thresholds in the retinal hazard region using lasers and shows the variety of different animal tissue and laser irradiation used. King and Geeraets[35] introduced the method of using animal tissue inside 'rose chambers', which are small containers or sample holders, to determine thresholds of Q-switched ruby lasers in 1968. Kelly's[36,37] studies are 'on the microcavitation and laser effects within RPE tissue samples and single melanosomes (porcine and bovine)'.[36] In 1999 Payne et al.[38] developed optical setups with an artificial retina to determine thresholds. In the same year methods of ex-vivo experiments were expanded by using rabbit tissue, as the fourth animal tissue in addition to porcine, bovine and chicken tissue. Laser tissue interaction mechanisms were investigated and ED_{50} values determined using this kind of optical setups with different parameter sets. The results of Brinkmann et al.[39] using single porcine melanosomes show that the 'origin of RPE cell damage for single pulse irradiation up to pulse durations of 3 ms can be described by a damage mechanism in which microbubbles around the melanosomes cause a rupture of the cell structure'.[39] In the following years research on the microbubble formation and the damage mechanism itself,[40,41] the detection of the laser-induced microbubbles[42] or damage thresholds caused by microbubble formation[13,40,43] was performed. A retinal in-vitro model was developed and cultured cells were irridiated by Denton et al.[44,45] with different wavelength scenarios. Schulmeister et al.[16,17,33,46] expanded the data base for the laser safety standard with extensive ex-vivo experiments on bovine explant tissue, termed ex-plant studies, in the visible and near infrared wavelength to validate the computer models of their research. Hutfilz et al. ,[14] Seifert et al. ,[47] Lipp et al. [15] and Herbst et al. [27] had different approaches on special parameter sets such as the pulse duration or multi pulse aspects with porcine tissue.

Provided that the transfer from porcine tissue to the human eye is successful,[27] the method of ex-vivo damage experiments is an alternative to in-vivo experiments on NHPs to determine retinal damage thresholds and explore laser tissue interaction mechanisms.

2.2 Process of ex-vivo experiments to determine retinal damage thresholds

The process of performing ex-vivo experiments is described in Fig. 2 in chronological sequences and refers to a previous work by Herbst et al.[27] Porcine eyes, that are leftovers from the slaughter, are delivered chilled from local slaughterhouses. Through an equatorial incision with cuttlery, the eyes are opened, the sensory part of the retina is removed and the tissue samples are placed in sample holders. The retinal pigment epithelium (RPE) and underlying layers are irradiated with an optical setup and exposed to a specific irradiation scenario. Within the irradiation process, the pulse energy is measured with calibrated measurement equipment for each individual exposure. The subsequent determination of whether a lesion or damage has occurred at the respective measuring point is achieved by staining, fluorescence imaging of the sample and subsequent image and statistical evaluation.

2.3 Statistical analysis and dose-response data

The statistical evaluation as the last process step of the ex-vivo experiments (Fig. 2) includes the creation of a dose-response curve and the results are therefore referred to as dose-response data. In the field of laser safety and retinal damage thresholds, a Probit analysis[48] is usually performed and a log-normal cumulative distribution is assumed for the dose-response curve. This log-normal distribution yields two important parameters, the slope and the median. The latter is referred to as the ED_{50} value. An 'accepted convention'[18] is to quote the ED_{50} value as an indication limit of retinal damage. Therefore, the ED_{50} value marks a reference point for laser damage evaluation. This type of analysis forms the basis for the definition of laser safety thresholds and risk analysis done for laser safety.[1,34]

To conclude, a 'dose-response curve describes the biological variation of the individual thresholds in a population'.[34] The spread of the threshold values within the dose-response curve originates from the 'spread of

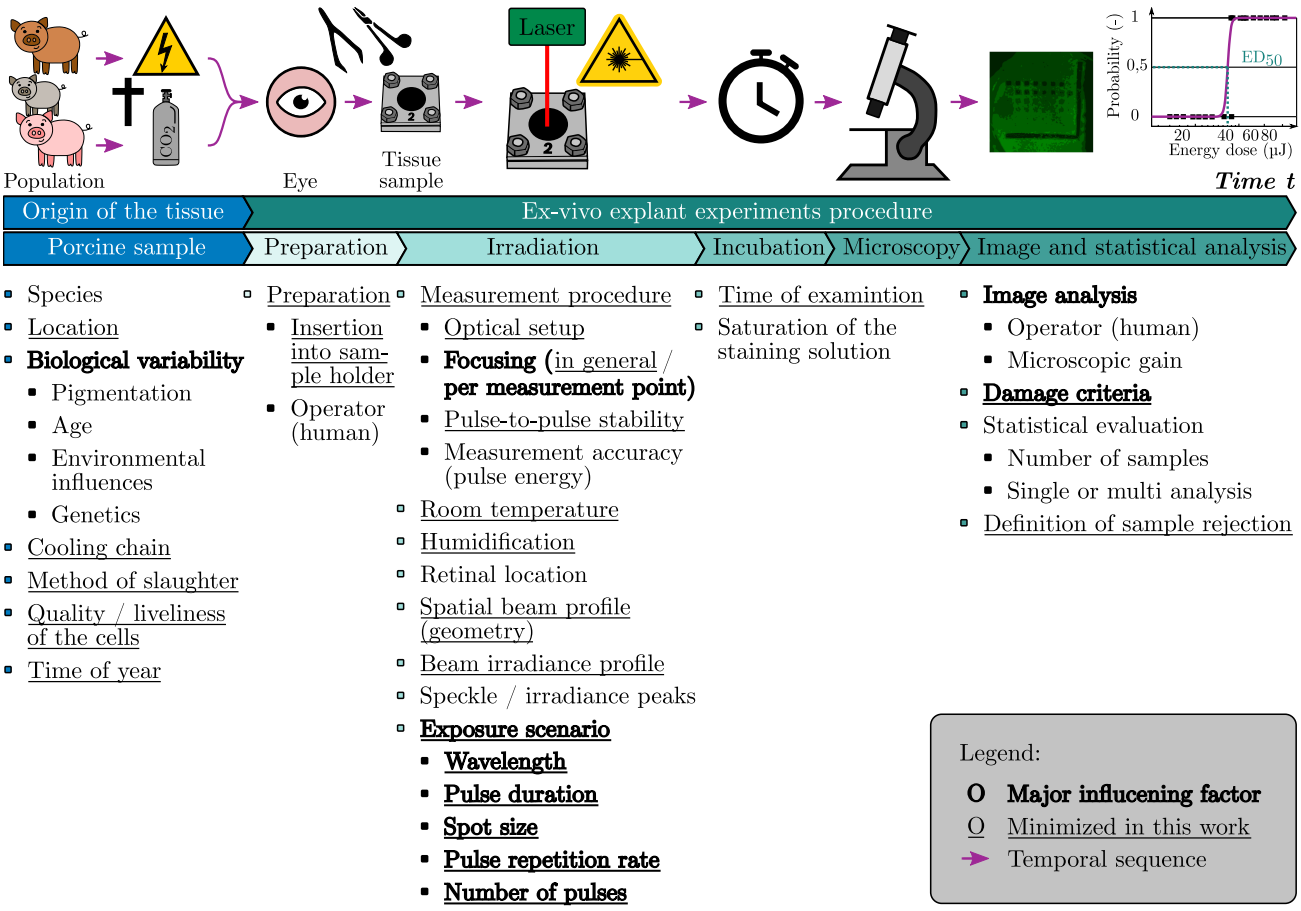

Figure 2. Schematic overview of the timeline of ex-vivo experiments from left to right. The corresponding influencing factors and influencing parameters of the exposure scenario on ex-vivo experiments with animal tissue are arranged below the respective process step. To determine ED_{50} values within ex-vivo experiments, porcine eyes are used. The process contains the following steps in this order: Preparation, irradiation, incubation, microscopy and image and statistical analysis. Major influencing factors determined within this and a previous work[27] are printed in bold font, whereas minor influencing factors are just written down. The influencing factors minimized in this works are underlined. One key finding is that the irradiation process (second step of the ex-vivo experiments) has the most influencing factors attatched to it.

sensitivities for the different exposure sites'[2,3] among others. Also, the 'variability within the group of experimental animals, such as inter-individual variability of absorption of the ocular media, can influence the shape of the dose-response curve'.[34] Additionally, there is some level of experimental uncertainty, e.g. in the correct focusing, within measurements and experiments for laser induced injury. These and other properties or uncertainties are inherent in the slope of the dose-response curve.[49] Therefore the slope has 'generally been considered a good indication of the overall uncertainty and quality of the experimental data'.[18]

2.4 Influencing factors of ex-vivo experiments to determine retinal damage thresholds

Sliney et al.[18] analized the major sources of uncertainties in in-vivo experiments with NHPs to experimentally determine dose-response data for retinal thermal injury (Tab. 1). In the work at hand the influencing factors or uncertainties of ex-vivo experiments with animal tissue are elaborated on the basis of this and a previous work[27] and listed in Fig. 2 below the temporal sequence. The relevance of the uncertainties by Sliney et al.[18] is evaluated in the context of ex-vivo experiments in the third column of Table 1.

The uncertainties Sliney et al.[18] evaluated are the time of examination, the animal model (species in this work), retinal pigmentation, retinal location, observer skills and lesion detection and beam quality, which are

Table 1. Analysis of the major sources of uncertainties in threshold and dose-response curve data of in-vivo experiments for retinal thermal injury by Sliney et al.[18] The impact of the respective influencing factor is presented for thermal injury and the relevance for ex-vivo experiments is stated.

Influencing factor for thermal retinal damage [Term in this work]	Impact for thermal retinal injury (n/a - not available)	Relevant to ex-vivo experiments
Time of examination	Factor of ∼1.2[18]	Yes
Animal model [Species]	n/a	Yes
Retinal Pigmentation	No big impact on the dose-response data	Yes
Observer skills and lesion detection [Image analysis, operator]	n/a	Yes
Beam quality	n/a	Yes
Retinal location	Factor of ∼2.0[50,51]	Yes
Eye movements	Only relevant for exposures >10 ms	No
Refractive state	Critical	No
Intraocular scatter	n/a	No
Biological variation [Biological variability]	n/a	Yes

relevant for ex-vivo measurements. Definitely not relevant are eye movements, the intraocular scatter and the refractive state, since the sample only consists of a flat tissue sample and the anterior parts of the eye are removed for ex-vivo measurements with explant tissue (Tab. 1).

Sliney et al.[18] stated that the time delay between laser irradiation and examination is critical for the process. For thermal injury a impact of 1.2 or less can be concluded by Sliney et al.[18] In other in-vivo experiments by Zuclich et al.[7] larger factors between 1 and 2 and sometimes > 2 resulted within the time differences of 1 hour or 24 hour post exposure readings. But a 24 hour post exposure reading or examination in ex-vivo experiments is not meaningful, because no biological regenerative processes inside an living organism take place.

The actual location of the retinal exposure will influence the ED_{50} value. Sliney et al.[18] lists the variability of the retinal location for thermal injury with a factor of 2.[50,51] This equals the results Zuclich et al.[7] got in their investigations on NHPs, where thermomechanical or microcavitation damage mechanisms should dominate. A conclusion is that, the ED_{50} values will be smaller in the fovea or macular regions than in paramacular regions.[7,18,50]

A major influencing factor is the operator, who applies the damage criteria for the analysis itself. For in-vivo experiments the 'experimental investigator observing the retina to detect a just-perceptible minimum visible lesion (MVL) also influences the ED_{50}'.[18] The task to determine a lesion is difficult through a slit-lamp in in-vivo experiments. In ex-vivo experiments the operator influences the analysis as well since the definition of a living or dead cell may vary on his visual impression and his settings of the microscope's software.

2.5 Biological variability and variation

In statistics, the variability defines the extent to which measurement or data points in a statistical distribution vary from the average value of this distribution and furthermore the extent to which these measurement points differ from each other. Gupta[52] defines the biological variation as 'the appearance of differences in the magnitude of response among individuals in the same population given the same dose of a compound'[52] in toxicology, which suits the term biological variability in this work well. In clinical chemistry or medicine the term biological variation is commonly used.[53] Both terms biological variation and variability have been used in laser damage specific literature in an equivalent way.[18,34] For this work the biological variability or variation is defined as the extent to which a response among the tissue samples in the same population varies given the same

dose of radiation. A definition with the same meaning is, that the probability distribution or dose-response curve describes the biological variability of the population for laser induced retinal damage together with the uncertainties of the process and measurements. Here, it has been noted by Schulmeister et al.[34] that there is a difference between a 'probability distribution describing biological variability [...][and] a probability distribution describing aleatory [, which means randomly based], i.e. stochastic uncertainty'.[34] A dose-response curve of a laser damage experiment should therefore not be interpreted in a mathematical way.

Each individual measurement point or site in retinal damage measurements has a given specific sharp threshold. In theory injury occurs by exceeding the threshold each time, which is not possible, since a site on the retina can not be damaged twice. 'For each exposure to a given individual and a given site with a given (known) threshold dose, there is no randomness in the response',[34] unless certain damage mechanisms are probability dependent. However, retinal damage thresholds are determined from a population and thus a (biological) variability exists between the individual values.[34] So generally, the damage threshold of a population 'is no sharply defined threshold'.[2] That means that there is no exposure level below which no injuries occur and above which all exposures definitively lead to a lesion in a biological tissue because of the biological variability.

In the subject of laser damage experiments there exist two different types of biological variability, which are the interindividual variability and the intra-individual variability:[34]

- The interindividual variability is a difference between individuals within the population. E.g. this could be age related properties like the general transmission of the cornea, which changes with the age.
- The intra-individual variability defines differences within a physical or biological property of an individual within the population. This could be the size and structure of the RPE cells or the melanin density on the retina, which both vary with the retinal location (macula vs. periphery) within a single individual or organism.[54]

In this work four aspects and origins are listed in relation to the biological variability of porcine tissue samples (Fig. 2), which are the pigmentation of the retina, the age of the organism, environmental influences and the genetics. As mentioned as an example for the intra-individual variability, the pigmentation varies within the retinal location but also within organisms like the skin pigmentation as well. Secondly the age of the porcine tissue samples plays an important role. Environmental influences can lead to a change inside the cells or sub cell structures of the tissue, changing physical properties in different ways within the population. In this context, genetics or genetic predisposition is understood as the resistance to external influences such as laser radiation for example, which differs within the population.

Since many influencing factors, which affect the dose-response curve for laser induced ocular damage, are mentioned and described 'there will be some degree of uncertainty associated with the shape of the dose-response curve which truly characterizes the biological variability of the population under consideration.'[34] The important part is to understand that the measurement accuracies play a role as an uncertainty within the dose-response data as well.[49] Therefore, the difference between the biological variability and the uncertainties is highlighted at this point, because both are listed and defined as influencing factors in this work (Fig. 2).

To improve the method of ex-vivo experiments, a minimization of the influencing factors and parameters is aimed at. One key finding of the process (Fig. 2) and of the analysis of the influencing factors itself is, that experiments to determine the biological variability should be performed on a single day. Then, there is no variation within the cooling chain and temperature of the day, season etc. and the eyes are from a single pool of pigs from the same slaughterhouse. Secondly, the optical setups must deliver a sound basis over several hours of measurement procedures to achieve constant irradiance scenarios. The goal is to determine the total interindividual variability, which means in between porcine eyes, and biological variability within all the different tissue samples to further develop and gain information on the influencing factors.

3. METHODS

To determine the interindividual biological variability of the porcine tissue samples in ex-vivo explant experiments the sequence of process steps, illustrated in Fig. 2, is performed, which is described in detail in a previous work.[27] Porcine eyes from different organisms are randomly selected. Multiple tissue samples are processed in the same way. For these experiments, the porcine eyes are leftovers from the slaughter and were obtained from one single slaughterhouse (Emil Färber GmbH & Co. KG, Mengen, Germany). There, before the slaughtering the animals are stunned with CO_2 gas, so no electric shock is used. In both the CO_2 and electric methods, the tissue is exposed to certain external influences. The influence on the tissue samples by using CO_2 gas can be considered to be small. Electrocution as a slaughtering method definitely has a larger impact on the sensory parts of the eyes, because the death of the animal is induced with an electric shock.

3.1 Minimization of the influencing factors and parameters

To minimize the influencing factors of the experiment (underlined factors in Fig. 2) some additional measures are realized:

- All experiments are performed on a single day and only eyes from one slaughterhouse are used. The eyes are stored and delivered chilled in a single container, to achieve the optimum quality and liveliness of the cells. Therefore, animals from the same local region are used, so there is less differences in the environmental influences on the tissue samples itself (minimized factors: Location, cooling chain, quality / liveliness of the cells, time of year). Only single pulse exposures are performed to optimize and minimize the duration and to get more data in the shortest possible time period. All data was gathered within a time span of nine hours. During this duration the evaluation of the images did reveal similar conditions in terms of the liveliness of the cells and freshness of the eyes itself. Further, the number of evaluable measuring points did not decrease over the measurement day. These facts lead to the conclusion that the quality of the eyes and the tissue samples was stable and equally good throughout the measurement day.
- The single steps of the process itself, such as the handling, preparation and staining, are performed by the same operator with the identical equipment and cutlery in the same laboratory and timing is monitored critically. (minimized factors: Preparation, insertion into sample holder, humidification)
- No changes of the irradiation scenario and the optical setup itself (Sec. 3.2) are done throughout the measurement day or between the tissue samples. The optical setup respectively the beam profile and spot geometry proofed to be stable on the days before, to minimize the differences within the irradiation scenario of every measurement point. The optical parameters defining the single exposure scenario are kept equal in size (minimized factors and parameters: Measurement procedure, optical setup, spatial beam profile (definition / geometry), exposure scenario, wavelength, pulse duration, spot size, pulse repetition rate, number of pulses).
- The best beam irradiance profile is achieved by using a new optical fiber (minimized factor: Beam irradiance profile).
- Climatized laboratory space is used and the room temperature is hold stable at about 21°C (minimized factor: Temperature).
- Minimization of the influencing factor, termed focusing in general (Fig. 2), is achieved by implementing a focusing method, where the square spot geometry is reviewed with an industrial camera on a thin film metal sheeting.[27] (minimized factor: Focusing in general) But the influencing factor focusing per measurement point is not completely minimized and still plays a role, as the tissue samples sometimes tend to bulge in the sample holder, which can lead to the fact that not all measurement points are perfectly in focus.
- Only single pulse exposures are applied on each measurement point. Differences in pulse energy of the laser source or tolerances of the irradiance do not play an additional role as in multi pulse scenarios, where pulse-to-pulse stability of the light source is important. For these measurements the pulse energy is detected inline, so only the measurement accuracy of the calibrated measurement equipment play a role (minimized factor: Pulse-to-pulse stability).

- The image analysis is performed by the same operator to minimize the human influence. Since there are always differences in the handling of the microscope's software and application of the damage criteria, the influencing factor of the operator is estimated by comparing the evaluation of two independent operators (Sec. 4.2). Nevertheless, clearly defined damage criteria have been defined in the previous work[27] and are applied in this work. Thereby, the operator is provided with clear rules for decision-making and definition of sample rejection (minimized factors: Damage criteria, definitions of sample rejection).

3.2 Irradiation process and beam shaping of square spot geometry

A single pulse irradiation scenario, characterized in Table 2, is generated with the optical setup shown in Fig. 3, which is described in detail in a previous work by Herbst et al.[27] For measuring the pulse energy, the exact same, calibrated measurement equipment as in the work by Herbst et al.[27] is used, which is the detector head 'J-10MB-LE' in combination with the power meter 'LabMax-TOP' (Coherent, Inc., Santa Clara, California, USA). For the optical fiber, the 'FP150QMT-CUSTOM' (Thorlabs, Inc., Newton, New Jersey, USA) version with 5 meters length is used.

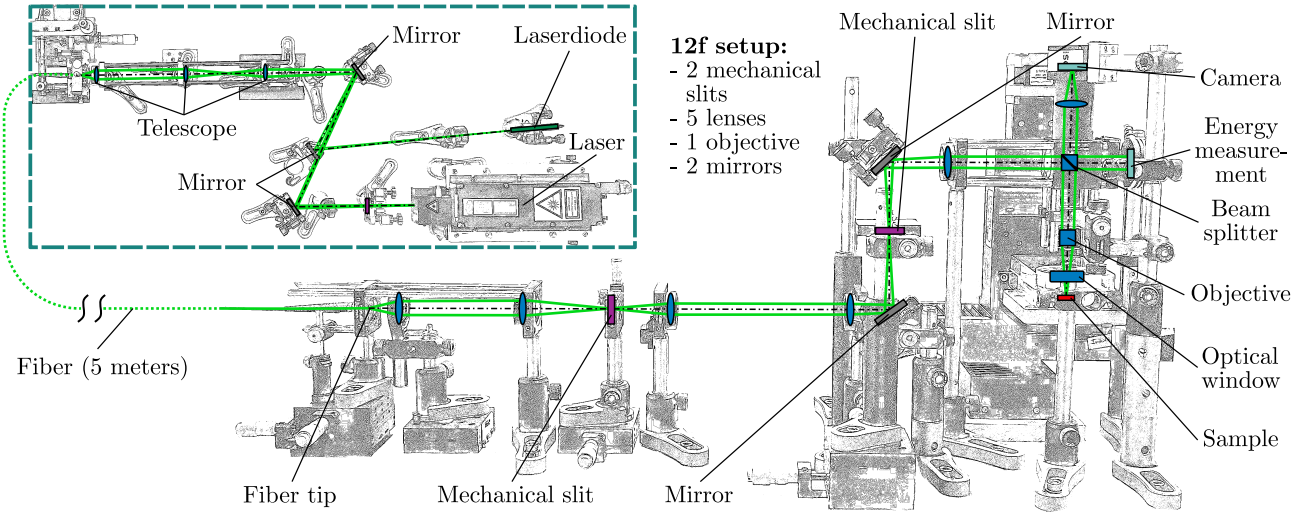

Figure 3. The optical setup used to irradiate tissue samples with a laser with 532 nm wavelength includes a 12f setup. The square spot geometry is shaped with the 12f setup, consisting of five lenses set up in their corresponding focal plane, two mirrors and two mechanical slits. The mechanical slits are set up in the focal plane between a pair of lenses and used as an aperture to vary the spot geometry in two dimensions (144.9 µm x 147.2 µm, Fig. 4).

Table 2. Parameters and measurands of the exposure scenario applied on the explant tissue samples (Further details of the measurements and type of measurement equipment see Herbst et al.[27])

Exposure scenario	Applied pulses per measurement point	Mean pulse duration	Peak wavelength	Spot size (Tophat)
Single pulse	1	2.23 ns	532.46 nm	144.9 µm x 147.2µm

The beam shaping of the square retinal spot geometry on the tissue sample is done with a 12f setup, in which the fiber tip of the optical fiber is imaged on the sample plane. Details of the optical equipment, such as lenses and objective, used can be found in a previous work.[27] Two mechanical apertures 'VA100/M' (Thorlabs, Inc., Newton, New Jersey, USA), mounted in the focal plane between an identical pair of lenses, allow variable adjustment of the rectangular spot geometry. For this work, the dimensions of the spot geometry are determined with the detector 'LaserCam-HR II - 1/2"'(Coherent, Inc., Santa Clara, California, USA) in the sample plane and adjusted by reviewing the image of the detector. The spatial distribution of the irradiance on the detector

in the sample plane is plotted in Fig. 4. The beam profile 'features a particular steep flank [...] and a strong definition of the irradiated area'.[27] A constant irradiance profile is achieved by mode mixing within the optical fiber.

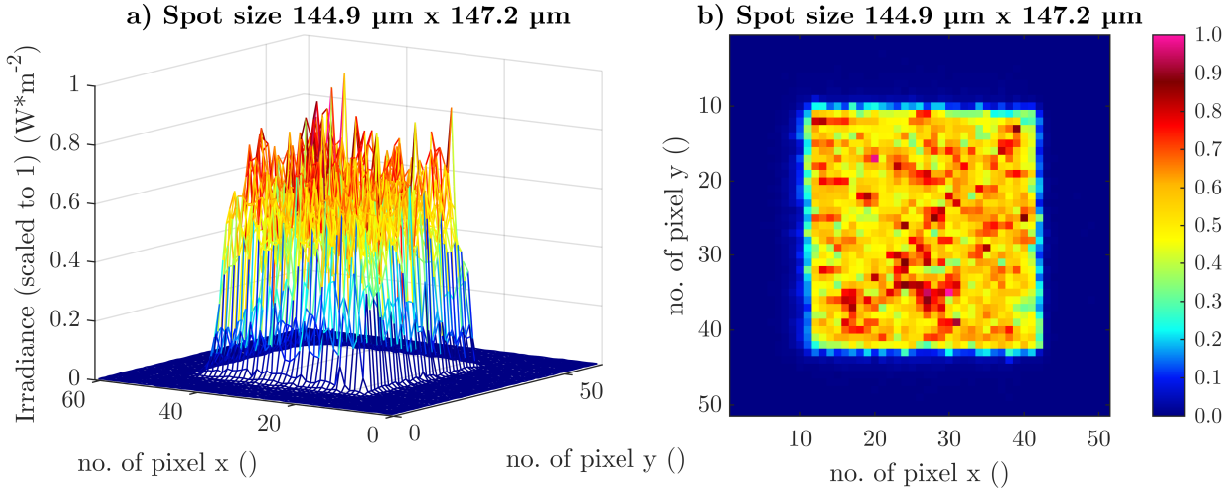

Figure 4. Characterization of the spatial beam profile for all tissue samples in the sample plane, plotted as irradiance of the beam profile in a three dimensional chart (a) and a two-dimensional chart (b). The sizes of the spot geometry is calculated with the manufacturer's information of the pixel size of 4.6 µm.

3.3 Image analysis and individual statistical analysis per sample

After the process of incubation with staining solution and the fluorescence microscopy, which are described in detail by Herbst et. al,[27] the image analysis is performed using the criteria defined in the previous work.[27] But in order to determine and estimate the effect of the human operator with respect to the image analysis, the image analysis is performed by two independent operators. These operators have clearly defined damage criteria and the same tools at their disposal, but e. g. an assessment of whether specific cells are alive or whether the measurement point is unevaluable is still subject to the subjective influence of the operator. In some cases, there are different nuances of the brightness of the staining of the cells or overlying dead cellular arrangements that influence the analysis of the tissue samples and the measurement points.

Unlike the previous work,[27] in which the statistical evaluation is only performed in a single dose-response curve for all the different tissue samples of the irradiation scenario, the statistical analysis is carried out individually per sample in addition (Fig. 5). Both methods, the statistical analysis with one dose-response curve, termed method ⓐ (Fig. 5(a)), and the individual analysis with individual dose-response curves per sample, termed method ⓑ (Fig. 5(b)), are performed. The statistical evaluation to determine the dose-response data is carried out with the 'ProbitFit' tool version 2.0 by Lund.[48] If the standard fitting procedure did not result in a suitable fit for the confidence intervals of 95 % probability, the 'Tolerance exponent' (default value: 9) is adjusted to a better fitting option within the software. For comparison, the statistical analysis is performed on a single basis for the method ⓐ with the sigmoidal fitting procedure 'DoseResp fit' using the software 'Origin version 2023b' (ADDITIVE Soft- und Hardware für Technik und Wissenschaft GmbH, Friedrichsdorf, Germany). For the individual statistical analysis method ⓑ, the binary information from the image analysis results in many dose-response curves with less measurement points for each curve.

3.4 Estimation and propagation of uncertainties

Further on, the term 'total variability' is defined as the differences of the individual tissue samples within the whole population of the experiment. Therefore, the total variability includes the influences of all the different influencing factors such as the biological variability and the measurement uncertainties.

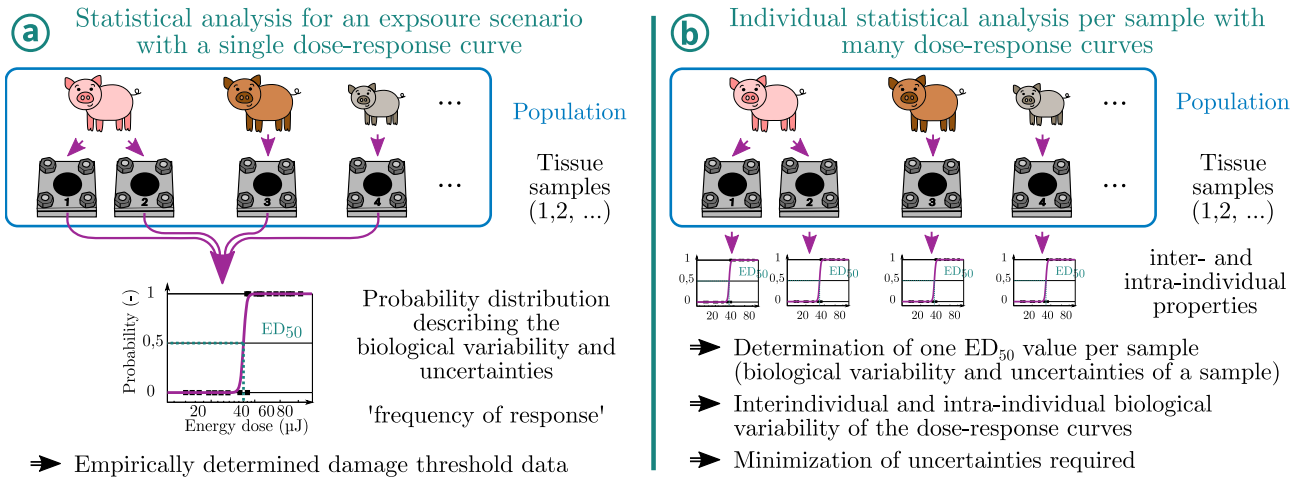

Figure 5. Overview of the two different statistical methods of analysis, which are the statistical analysis with a single dose-response curve for a given population (method ⓐ) and the individual statistical analysis per sample with one dose-response curve per sample (method ⓑ). The individual statistical analysis is performed in this work to determine inter- and intra-individual biological variability within the population, which includes a given set of tissue samples.

To determine the uncertainties of the two major influencing factors, biological variability and the focusing, a method based on the linear propagation of uncertainty is used. This method is also known as 'the sum of squares' method and is described by Eq. (1). It calculates the total uncertainty u_y of the function y. Therefore, the sum of squares of the partial derivatives of the function y for the linear independent input variables $x_i = x_1, x_2, \ldots$ and their individual uncertainties $u_i = u_1, u_2, \ldots$ are needed to calculate

$$u_y = \sqrt{\left(\frac{\partial y}{\partial x_1} \cdot u_1\right)^2 + \left(\frac{\partial y}{\partial x_2} \cdot u_2\right)^2 + \ldots} \,. \tag{1}$$

In addition, the assumption is made that linear independent uncertainties are present. Since no equation for the function y can be established for the whole ex-vivo experiments, an simplified approach is applied where the individual uncertainties $u_i = u_1, u_2, \ldots$ are estimated and calculated with the sum of squares.

4. RESULTS

4.1 Classical dose-response data: Statistical analysis with a single dose-response curve

Using the method ⓐ of statistical analysis (Fig. 5), all measurement points in total are evaluated in a single dose-response curve to gather one ED_{50} value as a reference. The results are listed in Table 3 for the two individual operators and for both software fitting options. In total, 753 measuring points can be evaluated from the experiments of the whole measurement day including 27 tissue samples, at which the criteria for an evaluation are fulfilled by the first operator. From the 27 tissue samples, one is discarded, because an error in the process of the alignment of the measurement rows in combination with focusing is detected. The number of measurement points evaluated by the second operator (821) does not match the first one's, because the image analysis includes criteria, where an operator must in- or exclude measurement points based on the staining of the cells or location of the damaged cells. Therefore, the procedure is dependent on the operator's skills, judgment and use of the software. In the following, the focus is on the results of the evaluation of the first operator. An estimation of the influence of a second, independent operator on the ED_{50} value is given later in the text. For comparison, another evaluation method with the software Origin is listed, because the evaluation with the 'ProbitFit' tool of the first operator did not result in confidence intervals with standard fitting parameters. Therefore, the 'Tolerance exponent' had to be adjusted from 9 to 3, which also influences the ED_{50} minimally (9.19 µJ shift to 9.17 µJ). Generally, the software fitting and settings of the fitting procedure have a minor influence on the ED_{50} and

are therefore belonging to the 'remaining minor influencing factors' in Sec. 4.3. However, since it is a common practice in the field of laser safety and the determination of retinal damage thresholds to use the ProbitFit tool, just the results with this tool will be further considered in the following for comparability.

Table 3. Dose-response data consisting of ED_{50} values from the ex-vivo measurements in µJ per pulse. The confidence limits (95%) of the statistical analysis are given in parentheses. The corresponding operator, tool, number of measurement days, number of porcine eyes and measurement points (M. points) involved or considered for the statistical analysis are listed. The slope is defined as the fraction of the ED_{84} and ED_{50} value. Parameters: wavelength: 532 nm; pulse duration: 2.2 ns; single pulses; evaluation after 1h.; measured spot size: 144.9 µm x 147.2 µm

Operator	Tool	Target spot size (µm^2)	Pulses	Days	Eyes	M. points	ED_{50} (µJ)	Slope
1	ProbitFit[48]	140x140	1	1	10	753	9.17 (8.92 - 9.42)	1.21
2	ProbitFit[48]	140x140	1	1	10	821	8.90 (7.86 - 9.80)	1.21
1	Origin	140x140	1	1	10	753	9.26 (9.14 - 9.39)	1.14
2	Origin	140x140	1	1	10	821	9.02 (8.88 - 9.15)	1.16

4.2 Image analysis, individual statistical analysis per sample and total variability

From the 26 tissue samples used for the statistical analysis with the method ⓐ including one single dose-resonse curve (Fig. 5), 25 can be evaluated within the method ⓑ with individual dose-reponse curves (Fig. 5) for the first operator's analysis. The excluded sample does not contain enough measurement points with and without a detected damage to perform a fit or an evaluation by the 'ProbitFit' tool by Lund[48] to create an individual dose-response curve. Nevertheless, 25 different single dose-response curves are created from 10 different porcine eyes. The ED_{50} values from the individual dose-response curves are plotted, grouped for the porcine eyes they originated from, in Fig. 6.

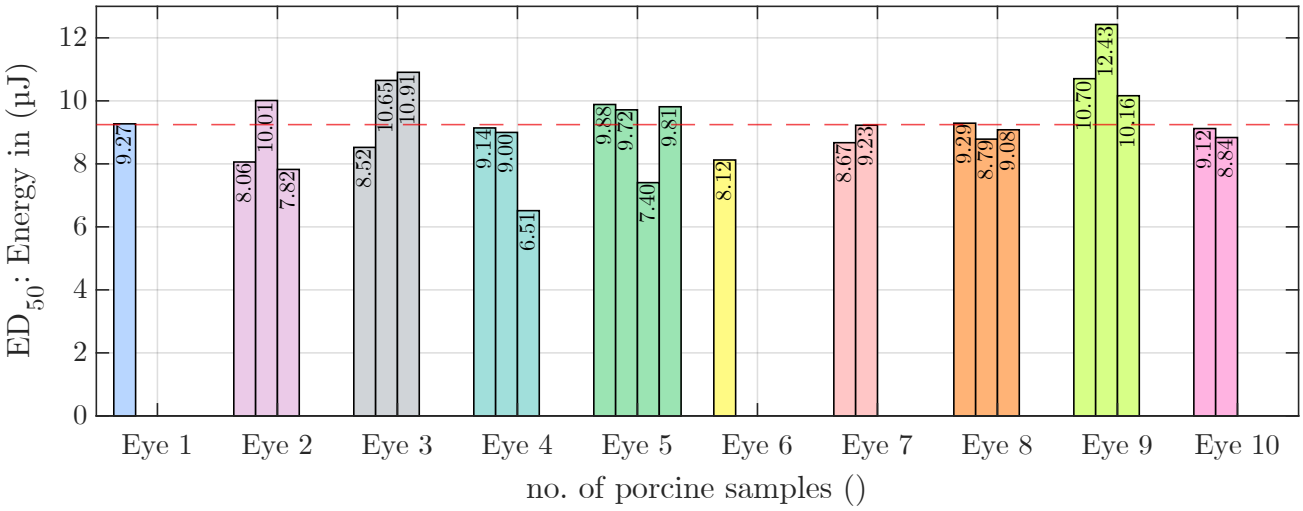

Figure 6. All ED_{50} values in µJ from the individual dose-response curves from all 25 porcine tissue samples with reference to the respective porcine eye for the first operator's analysis. The mean value ($\mu = 9.25$ µJ) is plotted with a dashed line.

Having a look on the total variability of the ED_{50} values of all 25 individual tissue samples, the maximum difference between the global minimum and maximum values (6.51 µJ and 12.43 µJ, between a sample from the eye 4 and 10) equals a spread of 5.92 µJ or a factor of 1.91 related to the mean value. The variability of the ED_{50} values between tissue samples within the same eye is smaller and the maximum value of the variability

within one eye equals a spread of 2.63 µJ or a factor of 1.40 for the first and third sample of the eye no. 4. The overview shows that there is quite some variability within all tissue samples, but the intra-individual variability within the same eye is much lower.

For the assessment of the intra-individual variability within porcine eyes of the ex-vivo experiments in this work in comparison to in-vivo experiments on NHP (factor of retinal location up to and equal to 2 with respect to the ED_{50} value, see Sec. 2.4), a closer look at the histological properties of the porcine eye is useful. A theory on the intra-individual variability could be that the 'visual streak'[55–57] in porcine eyes, which is the area of high density of photoreceptors, could influence the damage threshold in a way as it is done in NHP in-vivo experiments in regard to macular vs. paramacular irradiation. A variability this large within one eye can therefore be excluded for ex-vivo experiments based on the data generated in this work. Especially within the porcine eyes, where four or three tissue samples originated from, the factor of two should be recognizable. Since the eye is opened with a cut in the form of a cloverleaf with four leaves, this results in a maximum of four tissue samples per eye. Then, most likely one or two of them should contain the visual streak keeping its dimensions, schematically illustrated by Hendrickson and Hicks,[57] in mind.

In the following, the total variability or spread within the population consisting of all individual tissue samples is statistically assessed with a histogram of ED_{50} values evaluated according to method ⓑ (Fig. 5) performed by operator 1. For this purpose, the histogram is shown in Fig. 7. Based on the distribution a normal distribution is assumed and plotted with one and two-fold the standard deviation added to the mean (one and two-sigma intervals). The standard deviation has a value of $\sigma = 1.23\,\mu J$. The two-sigma interval limits determined on the basis of the statistical evaluation with the normal distribution is used to assess the total variability of the porcine tissue samples and the ex-vivo measurements. Therefore, the total variability or the total spread within this two-sigma interval is calculated with the upper and lower limit to be a value of 4.91 µJ. In the following, the assumption is made that all the single dose-response curve ED_{50} values, if correctly measured, should lie within this 95.4 % interval of the distribution and therefore describe the total variability. The mean value μ of this distribution is then set as the expected value z and the two-fold standard deviation $2 \cdot \sigma$ is defined as the total uncertainty. This would result in a value of $z = \mu \pm 2.46\,\mu J$ or $z = \mu \pm 26.58\%$, for the total variability, containing all the uncertainties and the biological variability.

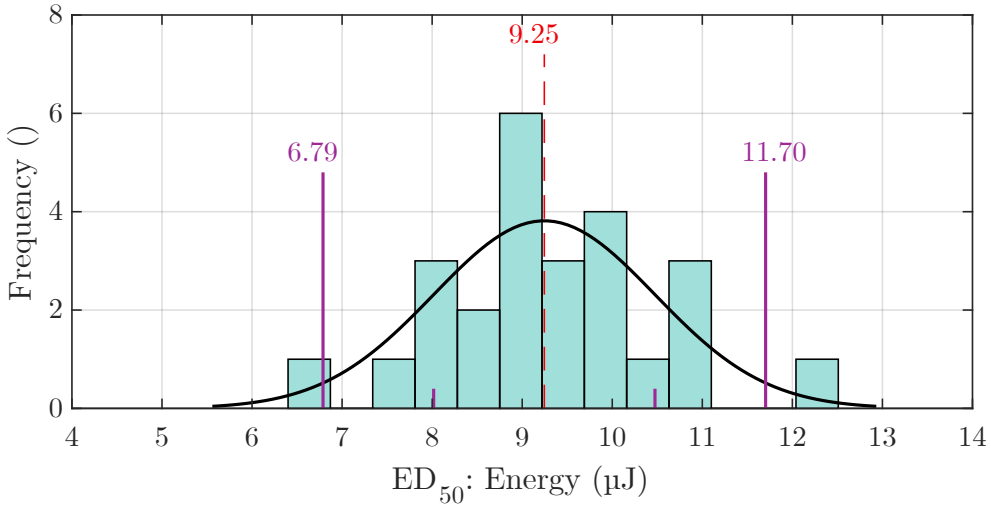

Figure 7. All ED_{50} values from the individual dose-response curves from a total of 25 porcine tissue samples in µJ plotted in a histogram. A normal distribution is fitted on top of the individual dose-response ED_{50} values and the corresponding two sigma interval is displayed. The mean value ($\mu = 9.25$ µJ) is plotted with a dashed line.

The influence of the operator performing the image analysis is shown in Table 3 for the analysis with one single dose-response curve (method ⓐ). The ED_{50} value of both individual operators is 8.90 µJ compared to 9.17 µJ. If method ⓑ is used by both operators, minor differences can be observed with respect to the ED_{50} values of

the individual dose-response curves from all the tissue samples. The individual evaluation in respect to the ED_{50} value is plotted in the appendix (Fig. 8). Some tissue samples contain different numbers of measurement points, which is why not every sample can be compared between the two operators, because a statistical dose-response curve could not be fitted every time. The influence of the operator is estimated on behalf of the resulting values of method ⓐ, where the difference in the ED_{50} value is estimated as an uncertainty (9.17 µJ - 8.90 µJ = 0.27 µJ). The worst case estimation is that this interval could be both in the positive and in the negative of the ED_{50}, since an operator could either have a restrictive or permissive judgment. Then this results in an value of $x = \mu \pm 2.99\%$, referenced to the mean of both operators' ED_{50} values.

To further determine the actual influence of the individual influcening factors such as the biological variability, every influencing factor will be reviewed and estimated in the following. In this way, an estimation can be made on how the total variability can be split up into the remaining influencing factors.

4.3 Influencing factors: Uncertainties and biological variability

An overview on the reviewed influencing factors and their contribution to the total variability is given with Table 4, derived from Fig. 2. In the first four rows the optical parameters of the setup are listed. The fifth and sixth row contains the influencing factors, which could or can be estimated and defined individually with values in this work. The seventh and eight row list the unknown major influencing factors.

Table 4. Overview of the influencing factors contributing to the ex-vivo experiments' total variability. The impact and values are listed based on calculations and estimations described or derived by means of a reference.

Influencing factor, contributing to the total variability	Impact (calculated or estimated)	Value	Comment, reference
Influencing factors: Measurement uncertainties of four optical parameters			
Uncertainty pulse energy measurement	Combination of powermeter and detector's uncertainty (sum of squares)	$x_1 = \mu \pm 2.2\%$	Reference: calibration sheet energy uncertainty (2.2 % at a 95 % confidence level ($k = 2$))
Wavelength dependency (worst case assumption)	Estimation with action spectra (Lund and Edsall,[30] ANSI, Seibersdorf)(±1.5 nm)	$x_2 = \mu \pm 0.53\%$	Reference: wavelength measurement (fit)[27] (FWHM: 2.52 nm)
Pulse duration stability	No impact, measurement's range below the thermal confinement time, small standard deviation	-	Reference: pulse duration measurement[27] (Standard deviation 39.26 ps)
Spot size	n/a	-	Included in the influencing factor 'Focusing'
Influencing factors: Estimations from this work			
Operator (image and statistical analysis)	Estimation on behalf of two individual operators	$x_3 = \mu \pm 2.99\%$	Reference: review of the two ED_{50} values of one statistical dose-response curve (Fig. 5(a))
Remaining minor influencing factors	No impact, can be neglected as an estimation, all minimized to a specific limit	-	-
Estimation of all major unknown influencing factors			
Biological variability + Focusing	Large impact, estimation using a simplified approach in this work	$x_4 = \mu \pm 26.31\%$	Minimization of the focusing: Set up of an autofocus system per measurement point required

Concerning the pulse measurement uncertainties, the manufacturer's calibration protocol for the combined uncertainty of the power meter and the detector lists a 2.2 % uncertainty at a given 95 % confidence level. The

combined uncertainty is received with the sum of squares method ($x_1 = \mu \pm 2.2\%$).

For the wavelength dependency a worst case assumption is made based on different sources listing thermal action spectra for retinal damage in the microsecond pulse regime, such as the action spectrum by Lund[30] and an 'ANSI 2021 plus model' as well as a 'Seibersdorf Laboratory Action Spectrum'. Such models result in a wavelength dependency on the ED_{50} with specific factors. Here, the 'ANSI 2021 plus model', which is rescaled to 530 nm, results in values of 0.9822 (525n̊m), 1 (530n̊m) and 1.0122 (535n̊m). The fit of the spectrometer software from the wavelength measurement of the optical setup resulted in a FWHM of 2.2 ns (see Herbst et. al[27]). This is why an interval of ± 1.5 ns is considered as a worst case assumption. Then, the worst case assumption equals a value with an uncertainty of $x_2 = \mu \pm 0.53\%$, if a linear approximation is assumed between these three wavelength factors.

Since the measurements are performed in the nano second time regime, where the pulse duration is below the thermal confinement time, it is assumed to neglect the uncertainty of the pulse duration as an influencing factor. In addition, the standard deviation of the pulse duration measured for the setup is very small (39.26 ps).

A varying spot size is the optical parameter related to the focusing on the sample. This is why this influencing factor is listed, but not evaluated as an individual aspect. It is included within the 'Focusing', since there is currently no assumption or estimation on it's impact possible. The focusing is minimized within the setup but an autofocus module (Sec. 5) may lead to better focusing for every single measurement point.

The operator's influence on the ED_{50} has been estimated within Sec. 4.2.

The remaining minor influencing factors, such as the operator's influence for the preparation, the speckle or irridiance peaks and number of tissue samples for the statistical analysis can be neglected, since these factors are all minimized within the procedure and kept equal within the experiments.

Table 4 lists the biological variability and focusing as major unknown influencing factors linked together, because for the given information of the optical setup and procedure they cannot be determined individually (Sec. 5). To estimate these major unknown influencing factors, the uncertainty u_4 of these influencing factors has to be calculated with a simplified approach from Sec. 3.4. Therefore, the Eq. (1) and the sum of squares method is used. The uncertainty u_4 is calculated to

$$u_4 = \sqrt{(u_z)^2 - (u_1)^2 - (u_2)^2 - (u_3)^2} \approx 2.43\,, \tag{2}$$

where u_1, u_2, u_3 are the individual uncertainties of the other influencing factors and u_z is the total uncertainty of the total variability. This results in an value of $x_4 = \mu \pm 2.43\,\mu J$ or $x_4 = \mu \pm 26.31\%$. On the basis of the chosen approach, this value is to be interpreted that the two major influencing factors, biological variability and focusing combined, result in a uncertainty or contribution to the ED_{50} in the amount of $\pm\,26.31\,\%$. This percentage is estimated with respect to the mean value μ of all individual dose-response curves of the tissue samples of the ex-vivo measurements (Fig.6). It can be derived, that the influencing factors, such as the uncertainties of the pulse energy measurement u_1, wavelength dependence u_2 and the operator's influence u_3 are much smaller than the uncertainty of the major unknown influencing factors combined in u_4, which is the biological variability and the focusing. Moreover, the estimation leads to the fact that the biological variability is assumed not to be greater than $\pm\,26.31\,\%$ for the given experiments on the single measurement day.

5. DISCUSSION

With the optical setup used for the ex-vivo experiments with porcine tissue samples, new single pulse retinal damage threshold data is generated. This work fully lists and estimates the influencing factors of the ex-vivo experiments for the first time and helps to further develop this method. The future goals can be a full recognition and usability of the retinal thresholds for upcoming complex irradiation scenarios, mentioned above, by laser safety committees. But therefore, the transfer to the human eye or NHP in-vivo measurements is still required. Nevertheless, this work provides guidance on the impact of the individual influencing factors and therefore gives important knowledge on the buildup of optical setups. An important finding is that a further minimization of the remaining influencing factors is required, especially for a determination of the biological variability as an

influencing factor itself. This can be achieved, for example, by implementing an autofocus system and determining the influence of the focusing separately. This will further improve the accuracy of ex-vivo experiments.

The approach to determine the total variability and the contribution of the influencing factors contains many assumptions and simplifications and is, however, the first of its kind. Therefore, restrictive worst case assumptions are made on purpose. With the important minimization of many influencing factors mentioned, the methods applied for the minimization themselves help to improve the accuracy of ex-vivo experiments. This approach can therefore be seen as a first step.

As mentioned in the previous work,[27] the need for a common practice of the procedure of ex-vivo experiments is high. This is the only way to obtain reliable results, which are important in order to gain acceptance and to be evaluated more quickly by the laser safety experts and committees. Then, the resulting ED_{50} values with a safety margin can be included in the proposed emission limit values of national or international standards. Only with stable and defined procedures and present reproducibility, the best comparability between the different experiments and parameter sets can be achieved. In this way, models of retinal damage and the mechanisms itself can be improved and created to gain information on the retinal damage mechanisms itself.

ACKNOWLEDGMENTS

The authors thank the staff of the Institute for Ophthalmic Research of the University Hospital Tuebingen, Germany, namely Sven Schnichels, Manuela Leinwetter and Armin Safaei, for supporting the sample preparation and fluorescence microscopy imaging. Moreover, the authors thank Brian Lund for providing the 'ProbitFit' software.

REFERENCES

[1] IEC 60825-1:2014, [*Safety of laser products - Part 1: Equipment classification and requirements*], International Electrotechnical Commission (2014).

[2] Henderson, R. and Schulmeister, K., [*Laser Safety*], CRC Press (Dec. 2003).

[3] Sliney, D. H., Mellerio, J., Gabel, V.-P., and Schulmeister, K., "What is the meaning of threshold in laser injury experiments? Implications for human exposure limits," *Health Physics* **82**, 335–347 (Mar. 2002).

[4] Ebbers, R. W., "Retinal effects of a multiple-pulse laser," *American Industrial Hygiene Association Journal* **35**, 252–256 (May 1974).

[5] Lund, D. J. and Beatrice, E. S., "Near infrared laser ocular bioeffects," *Health Physics* **82**, 335–347 (Mar. 2002).

[6] Cain, C. P., Toth, C. A., Noojin, G. D., Stolarski, D. J., Thomas, R. J., and Rockwell, B. A., "Thresholds for retinal injury from multiple near-infrared ultrashort laser pulses," *Health Physics* **82**, 855–862 (June 2002).

[7] Zuclich, J. A., Edsall, P. E., Lund, D. J., Stuck, B. E., Till, S., Hollins, R. C., Kennedy, P. K., and McLin, L. N., "New data on the variation of laser induced retinal-damage threshold with retinal image size," *Journal of Laser Applications* **20**, 83–88 (May 2008).

[8] Lund, B. J., Lund, D. J., Edsall, P. R., and Gaines, V. D., "Laser-induced retinal damage threshold for repetitive-pulse exposure to 100-μs pulses," *Journal of Biomedical Optics* **19**(10), 105006 (2014).

[9] Lund, D. J. and Lund, B. J., [*Laser-induced ocular effects in the retinal hazard region*], ch. 9, 171–186, Borden Institute, US Army Medical Center of Excellence (2020).

[10] Roider, J., Hifnawi, E.-S. E., and Birngruber, R., "Bubble formation as primary interaction mechanism in retinal laser exposure with 200-ns laser pulses," *Lasers in Surgery and Medicine* **22**(4), 240–248 (1998).

[11] Framme, C., Schuele, G., Roider, J., Kracht, D., Birngruber, R., and Brinkmann, R., "Threshold determinations for selective retinal pigment epithelium damage with repetitive pulsed microsecond laser systems in rabbits," *Ophthalmic Surgery, Lasers and Imaging Retina* **33**, 400–409 (Sept. 2002).

[12] Framme, C., Schuele, G., Kobuch, K., Flucke, B., Birngruber, R., and Brinkmann, R., "Investigation of selective retina treatment (SRT) by means of 8 ns laser pulses in a rabbit model," *Lasers in Surgery and Medicine* **40**, 20–27 (Jan. 2008).

[13] Brinkmann, R., Koop, N., Oezdemir, M., Alt, C., Schuele, G., Lin, C. P., and Birngruber, R., "Selective damage of pigmented cells by means of a rapidly scanned cw laser beam," in [*SPIE Proceedings*], Jacques, S. L., Duncan, D. D., Kirkpatrick, S. J., and Kriete, A., eds., SPIE (June 2002).

[14] Hutfilz, A., Burri, C., Meier, C., and Brinkmann, R., "Ex vivo investigation of different µs laser pulse durations for selective retina therapy," in [*Medical Laser Applications and Laser-Tissue Interactions IX*], Lilge, L. D. and Philipp, C. M., eds., SPIE (July 2019).

[15] Lipp, S., *Untersuchung der Augensicherheit durch Multi-Pulsbestrahlung für LiDAR-Anwendungen*, PhD thesis, Karlsruhe Institute of Technology (2021).

[16] Schulmeister, K., Husinsky, J., Seiser, B., Edthofer, F., Tuschl, H., and Lund, D. J., "Ex-plant retinal laser induced threshold studies in the millisecond time regime," in [*Optical Interactions with Tissue and Cells XVII*], Jacques, S. L. and Roach, W. P., eds., SPIE (Feb. 2006).

[17] Schulmeister, K., Seiser, B., Edthofer, F., Husinsky, J., and Farmer, L., "Retinal thermal damage threshold studies for multiple pulses," in [*SPIE Proceedings*], Manns, F., Soederberg, P. G., Ho, A., Stuck, B. E., and Belkin, M., eds., SPIE (Feb. 2007).

[18] Sliney, D. H., Mellerio, J., and Schulmeister, K., "Implications of using ED-50 and probit analysis in comparing retinal injury threshold data," in [*SPIE Proceedings*], Stuck, B. E. and Belkin, M., eds., SPIE (May 2001).

[19] Niemz, M. H., [*Laser-Tissue Interactions*], Springer International Publishing (2019).

[20] International Commission on Non-Ionizing Radiation Protection, "ICNIRP guidelines on limits of exposure to laser radiation of wavelengths between 180 nm and 1,000 µm," *Health Physics* **105**, 271–295 (Sept. 2013).

[21] Schulmeister, K., "Concepts in dosimetry related to laser safety and optical-radiation hazard evaluation," in [*SPIE Proceedings*], Stuck, B. E. and Belkin, M., eds., SPIE (May 2001).

[22] Yole Group, "LiDAR for Automotive and Industrial Applications 2021," techreport, Yole Group (2021).

[23] Neustadt, A., "Lidar sensor for the optical detection of a field of view working device or vehicle with a lidar sensor, and method for the optical detection of a field of view by means of a lidar sensor," (Mar. 2021).

[24] Maurer, T., Holleczek, A., Schnitzer, R., and Hipp, T., "Lidar sensor for optically detecting a field of view, working apparatus or vehicle having a lidar sensor, and method for optically detecting a field of view," (Feb. 2020).

[25] Spiessberger, S., "Optical system, in particular lidar system, and vehicle," (July 2020).

[26] Kotzur, S., Wahl, S., and Frederiksen, A., "Simulation of laser-induced retinal thermal injuries for non-uniform irradiance profiles and the applicability of the laser safety standard," *Optical Engineering* **60** (June 2021).

[27] Herbst, M., Kotzur, S., Frederiksen, A., and Stork, W., "Nanosecond Multipulse Retinal Damage Thresholds of Elongated Irradiance Profiles in Explant Measurements and Simulations, [currently being reviewed]," *Journal of Biomedical Optics* .

[28] Schulmeister, K., "Extended Source AEL Analysis of Scanned Laser Emission for IEC 60825-1," tech. rep., Seibersdorf Labor GmbH (Apr. 2023).

[29] Lund, D. J., Stuck, B. E., and Beatrice, E. S., "Biological research in support of project miles.," tech. rep., Letterman Army Inst. of Research San Francisco CA (1981).

[30] Lund, D. J. and Edsall, P. R., "Action spectrum for retinal thermal injury," in [*SPIE Proceedings*], Rol, P. O., Joos, K. M., Manns, F., Stuck, B. E., and Belkin, M., eds., SPIE (June 1999).

[31] Heussner, N., Ramos, S., Lücking, M., Schwarz, C., and Frederiksen, A., "Eye safety evaluation of laser systems based on damage calculations," in [*International Laser Safety Conference*], Laser Institute of America (2019).

[32] Heussner, N., Holl, L., Nowak, T., Beuth, T., Spitzer, M. S., and Stork, W., "Prediction of temperature and damage in an irradiated human eye – Utilization of a detailed computer model which includes a vectorial blood stream in the choroid," *Computers in Biology and Medicine* **51**, 35–43 (Aug. 2014).

[33] Schulmeister, K., Husinsky, J., Seiser, B., Edthofer, F., Fekete, B., Farmer, L., and Lund, D. J., "Ex vivo and computer model study on retinal thermal laser-induced damage in the visible wavelength range," *Journal of Biomedical Optics* **13**(5), 054038 (2008).

[34] Schulmeister, K., Sonneck, G., Hoedlmoser, H., Rattay, F., Mellerio, J., and Sliney, D. H., "Modeling of uncertainty associated with dose-response curves as applied for probabilistic risk assessment in laser safety," in [*SPIE Proceedings*], Stuck, B. E. and Belkin, M., eds., SPIE (May 2001).
[35] King Jr., R. G. and Geeraets, W. J., "The effect of q-switched ruby laser on retinal pigment epithelium in vitro," *Acta Ophthalmologica* **46**(4), 617–632 (1968).
[36] Kelly, M. W., *Intracellular cavitation as a mechanism of short-pulse laser injury to the retinal pigment epithelium*, PhD thesis, Tufts university (1997).
[37] Kelly, M. W. and Lin, C. P., "Microcavitation and cell injury in rpe cells following short-pulsed laserirradiation," in [*Laser-Tissue Interaction VIII*], Jacques, S. L., ed., SPIE (June 1997).
[38] Payne, D. J., Jost, T. R., Elliot, J. J., Eilert, B., Lott, L., Lott, K., Noojin, G. D., Richard A. Hopkins, J., Lin, C. P., and Rockwell, B. A., "Cavitation thresholds in the rabbit retinal pigmented epithelium," in [*SPIE Proceedings*], Jacques, S. L., Mueller, G. J., Roggan, A., and Sliney, D. H., eds., SPIE (June 1999).
[39] Brinkmann, R., Hüttmann, G., Rögener, J., Roider, J., Birngruber, R., and Lin, C. P., "Origin of retinal pigment epithelium cell damage by pulsed laser irradiance in the nanosecond to microsecond time regimen," *Lasers in Surgery and Medicine* **27**(5), 451–464 (2000).
[40] Schüle, G., *Mechanismen und On-line Dosimetrie beiselektiver RPE Therapie*, PhD thesis, Universität zu Lübeck (Jan. 2003).
[41] Neumann, J. and Brinkmann, R., "Nucleation and dynamics of bubbles forming around laser heated microabsorbers," in [*SPIE Proceedings*], van den Bergh, H. and Vogel, A., eds., SPIE (June 2005).
[42] Roegener, J., Brinkmann, R., and Lin, C. P., "Pump-probe detection of laser-induced microbubble formation in retinal pigment epithelium cells," *Journal of Biomedical Optics* **9**(2), 367 (2004).
[43] Schuele, G., Rumohr, M., Huettmann, G., and Brinkmann, R., "RPE damage thresholds and mechanisms for laser exposure in the microsecond-to-millisecond time regimen," *Investigative Opthalmology & Visual Science* **46**, 714 (Feb. 2005).
[44] Denton, M. L., Foltz, M. S., Estlack, L. E., Stolarski, D. J., Noojin, G. D., Thomas, R. J., Eikum, D., and Rockwell, B. A., "Damage thresholds for exposure to NIR and blue lasers in an in vitro RPE cell system," *Investigative Opthalmology & Visual Science* **47**, 3065 (July 2006).
[45] Denton, M. L., Tijerina, A. J., Dyer, P. N., Oian, C. A., Noojin, G. D., Rickman, J. M., Shingledecker, A. D., Clark, C. D., Castellanos, C. C., Thomas, R. J., and Rockwell, B. A., "Evidence of thermal additivity during short laser pulses in an in vitro retinal model," in [*SPIE Proceedings*], Jansen, E. D., ed., SPIE (Mar. 2015).
[46] Schulmeister, K., Ullah, R., and Jean, M., "Near infrared ex-vivo bovine and computer model thresholds for laser-induced retinal damage," *Photonics & Lasers in Medicine* **1** (Jan. 2012).
[47] Seifert, E., Sonntag, S. R., Kleingarn, P., Theisen-Kunde, D., Grisanti, S., Birngruber, R., Miura, Y., and Brinkmann, R., "Investigations on retinal pigment epithelial damage at laser irradiation in the lower microsecond time regime," *Investigative Opthalmology & Visual Science* **62**, 32 (Mar. 2021).
[48] Lund, B. J., "The probitfit program to analyze data from laser damage threshold studies," tech. rep., Northrop Grumman Corporation, Walter Reed Army Institute of Research, San Antonio, TX 78228 (May 2006).
[49] Husinsky, J., *Experimental ex-vivo studies of laser-induced thermal damage of the bovine retina for single pulse, multiple pulse, and scanned exposures to improve laser safety standards*, PhD thesis, Technische Universität Wien (2008).
[50] Lappin, P. W. and Coogan, P. S., "Relative sensitivity of various areas of the retina to laser radiation," *Archives of Ophthalmology* **84**, 350–354 (Sept. 1970).
[51] Beatrice, E. S., Randolph, D. I., Zwick, H., Stuck, B. E., and Lund, D. J., "Laser Hazards: Biomedical Threshold Level Investigations," *Military Medicine* **142**, 889–891 (11 1977).
[52] Gupta, P., "General toxicology," in [*Illustrated Toxicology*], Gupta, P., ed., 1–65, Elsevier (2018).
[53] Aarsand, A. K., Røraas, T., Fernandez-Calle, P., Ricos, C., Díaz-Garzón, J., Jonker, N., Perich, C., González-Lao, E., Carobene, A., Minchinela, J., Coşkun, A., Simón, M., Álvarez, V., Bartlett, W. A., Fernández-Fernández, P., Boned, B., Braga, F., Corte, Z., Aslan, B., and Sandberg, S., "The biological variation data critical appraisal checklist: A standard for evaluating studies on biological variation," *Clinical Chemistry* **64**, 501–514 (Mar. 2018).

[54] Boulton, M. and Dayhaw-Barker, P., "The role of the retinal pigment epithelium: Topographical variation and ageing changes," *Eye* **15**, 384–389 (May 2001).

[55] Barone, F., Nannoni, E., Elmi, A., Lambertini, C., Scorpio, D. G., Ventrella, D., Vitali, M., Maya-Vetencourt, J. F., Martelli, G., Benfenati, F., and Bacci, M. L., "Behavioral assessment of vision in pigs," *Journal of the American Association for Laboratory Animal Science* **57**, 350–356 (July 2018).

[56] Wagner, N., Reinehr, S., Gammel, M. R., Greulich, A., Hurst, J., Dick, H. B., Schnichels, S., and Joachim, S. C., "Novel porcine retina cultivation techniques provide improved photoreceptor preservation," *Frontiers in Neuroscience* **14** (Oct. 2020).

[57] Hendrickson, A. and Hicks, D., "Distribution and density of medium- and short-wavelength selective cones in the domestic pig retina," *Experimental Eye Research* **74**, 435–444 (Apr. 2002).

[58] Payne, D. J., Hopkins, R. A., Eilert, B. G., Noojin, G. D., Stolarski, D. J., Thomas, R. J., Cain, C. P., Hengst, G. T., Kennedy, P. K., Jost, T. R., and Rockwell, B. A., "Comparative study of laser damage threshold energies in the artificial retina," *Journal of Biomedical Optics* **4**(3), 337 (1999).

[59] Lee, H., Alt, C., Pitsillides, C. M., and Lin, C. P., "Optical detection of intracellular cavitation during selective laser targeting of the retinal pigment epithelium: dependence of cell death mechanism on pulse duration," *Journal of Biomedical Optics* **12**(6), 064034 (2007).

APPENDIX

Table 5. Overview of literature on ex-vivo tissue experiments with laser-induced damage in the retinal hazard region. Abbreviations: A: Artificial, C: Chicken, P: Porcine, B: Bovine, R: Rabbit, HC: Human cell lines, RPE: RPE tissue, M: Single melanosomes, AR: Artificial retina, CE: Single RPE cells, CF: RPE cell fragments, IVM: In-vitro model, SRT: Selective retinal therapy

First author	Year	Animal	Sample	Wavelength (nm)	Goal / research topic
King[35]	1968	C	RPE	694.3	Thresholds of Q-switched laser irradiation
Kelly[36,37]	1997	P, B	M, RPE	532, 1064	Studies on microcavitation and laser effects
Payne[38]	1999	A	AR	532, 580, 1064	Determine thresholds on an artificial retina
Payne[58]	1999	R, P	RPE	532, 580	Determine ED_{50} values
Brinkmann[39]	2000	P	M, RPE	527, 532	Microcavity mechanism, Determine ED_{50} values
Brinkmann[13]	2002	P	RPE	514	Scanning laser exposure, Determine ED_{50} values
Schuele[40]	2003	P	RPE	514, 527, 532	Non-invasive on-line dosimetry for SRT
Rögener[42]	2004	P	CE	532	Detection of laser-induced microbubbles
Neumann[41]	2005	P	CE, CF	527, 532	Bubble dynamics in RPE tissue
Schuele[43]	2005	P	RPE	514	RPE Damage Thresholds
Denton[44]	2006	HC, B	IVM	458, 810	Damage thresholds in an in vitro cell system
Schulmeister[16]	2006	B	RPE	532	Ex-plant retinal laser induced threshold studies
Schulmeister[17]	2007	B	RPE	532	Ex-plant retinal laser induced threshold studies
Lee[59]	2007	B	RPE	532	Intracellular cavitation, Determine ED_{50} values
Schulmeister[33]	2008	B	RPE	532	Validation of computer model (bovine, ex-vivo)
Schulmeister[46]	2012	B	RPE	1090	Near infrared computer model
Denton[45]	2015	HC, B	IVM	532	Short laser pulses in an in-vitro retinal model
Hutfilz[14]	2019	P	RPE	532	Studies on pulse durations for SRT
Seifert[47]	2021	P	RPE	514	RPE damage thresholds and mechanisms
Lipp[15]	2021	P	RPE	532	Multipulse laser induced retinal damage
Herbst[27]	2023	P	RPE	532	Multipulse laser induced retinal damage

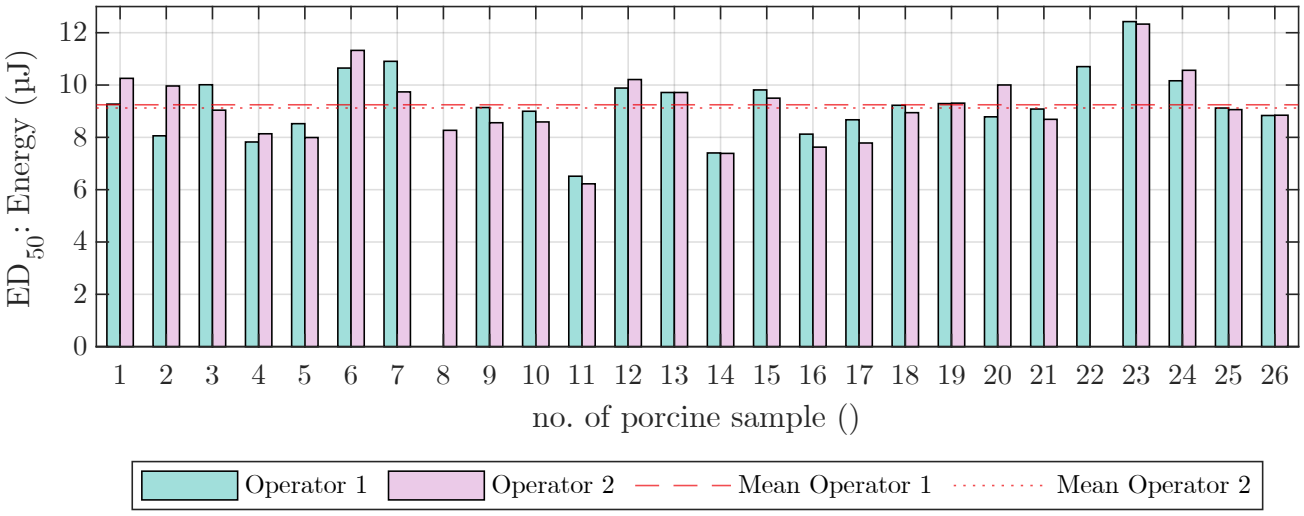

Figure 8. All ED_{50} values from the individual dose-response curves from a total of 26 porcine tissue samples in µJ in regard to the image analysis performed by two individual operators. The mean values (operator 1: $\mu_1 = 9.25$ µJ, operator 2: $\mu_2 = 9.12$ µJ) are plotted dashed and dotted.